APPLICATION OF HUMAN TRANSFER FUNCTIONS TO A DESIGN PROBLEM

By James J. Adams

NASA Langley Research Center
Langley Station, Hampton, Va.

Presented at the USC-NASA Conference on Manual Control
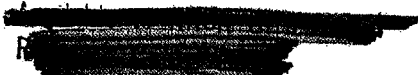
Los Angeles, California
March 1-3, 1967

███████████████

APPLICATION OF HUMAN TRANSFER FUNCTIONS TO A DESIGN PROBLEM

By James J. Adams

NASA Langley Research Center

SUMMARY

An analytical design study was made of a proposed full-scale, manually controlled lunar landing simulator using analytical transfer functions for the pilot control response along with the analytical representation for the mechanisms. The simulator reproduced the lunar environment by supporting five-sixths of the weight of the test vehicle with an overhead cable. The cable was kept directly over the test vehicle by the automatic control of the longitudinal drive mechanism of the simulator. The results showed that the dynamic characteristics of the simulator that could be expected in the actual system were in a range that would influence the response of the manually controlled systems which were to be tested.

When the simulator was put in operation, the results of the analytical study were checked. The simulator was operated with the gain of the longitudinal drive set as high as was feasible with the actual mechanism and with a low gain to determine if this change would affect the pilot's response. The pilots reported that the degraded system was more difficult to control, and the records clearly showed a decrease in system damping with the degraded system.

INTRODUCTION

One of the reasons for determining human transfer functions is so that evaluation and prediction of the performance of manually controlled systems

L-5470

can be accomplished during design studies. This report explains how such transfer functions were used in the design analysis of the drive system of a lunar landing simulator.

The simulator was designed to provide a 400-foot by 50-foot by 180-foot high volume in which lunar landing maneuvers could be studied. The lunar gravity was simulated by supporting five-sixths of the weight of the test vehicle by a cable. The load in the cable was regulated by measuring the load with a strain gage and operating the overhead winch in response to the error in this measured load. The cable was kept directly over the vehicle by measuring the cable angle at the overhead, traveling bridge, and moving the bridge in response to this measured angle. It is this longitudinal drive system of the bridge that is the subject of the design study reported in this paper.

The transfer functions used to describe the pilot's control action were derived in reference 1. These transfer functions describe the pilot's control used when controlling the multiloop system representative of the lunar landing horizontal translation maneuver. The use of these pilot transfer functions in determining the most suitable simulator drive characteristics will be presented.

SYMBOLS

m	mass, slugs
x	translation, ft (m)
l	pendulum length, ft (m)
φ	pendulum angle, deg
g	gravity, 32.2 ft/sec^2 (9.81 m/sec^2)
$K_\varphi, K_{\dot{\varphi}}$	simulator drive system control gains
s	LaPlace operator, per second

θ	pitch attitude angle, deg
δ	control moment, rad/sec^2
ω	undamped natural frequency, rad/sec
h	maximum deflection of first cable vibration mode, ft (m)
K_1, K_2, τ	gains in analytical transfer function of pilot
Q_L	leakage flow, in^3/sec
Q_{RL}	relief valve flow, in^3/sec
V	oil volume under compression, in^3
B	bulk modulus of oil, psi
P_m	motor pressure, psi
D_m	motor volume, in^3
J_m	motor inertia, $in\text{-}lb\text{-}sec^2$
ω_m	motor rotation, rad/sec
n	gear ratio
B_m	motor damping, $in\text{-}lb/rad/sec$
K_L	tire torsional spring constant, $in\text{-}lb/rad$
T_L	tire torque, lb
J_L	load inertia, $in\text{-}lb\text{-}sec^2$
B_L	load visious friction, $in\text{-}lb/rad/sec$

Subscripts:

B	bridge
V	vehicle
c	command
e	error

DESCIPTION OF PROBLEM

Simulator

Simplified equations of motion for the longitudinal motion of the over-head bridge and pendulum consisting of the cable-supported vehicle are:

$$\left(m_B + m_V\right)\ddot{x}_B + m_V l\ddot{\varphi} = 0$$

$$m_V l\ddot{x}_B + m_V l^2\ddot{\varphi} + m_V gl\varphi = 0$$

The characteristic equation for the system in LaPlace rotation is

$$\left(m_B + m_V\right)\left(m_V l^2\right)s^2 + \left(m_B + m_V\right)\left(m_V gl\right) - m_V^2 l^2 s^2 = 0$$

which is the familiar equation for a pendulum in which the frequency is primarily determined by the length 1 but with an additional term which represents the influence of the bridge being free to move, which reduces the frequency somewhat.

If the control commands that the bridge accelerates as a function of φ and $\dot{\varphi}$ then the equations of motion become:

$$\left(m_B + m_V\right)\ddot{x}_B + m_V l\varphi = -K_\varphi\varphi - K_{\dot{\varphi}}\dot{\varphi}$$

$$m_V l\ddot{x}_B + m_V l^2\ddot{\varphi} + m_V gl\varphi = 0$$

The characteristic equation, in LaPlace rotation, is:

$$\left(m_B + m_V\right)\left(m_V l^2\right)s^2 + \left(m_V l K_{\dot{\varphi}}\right)s + \left(m_B + m_V\right)\left(m_V gl\right) - m_V^2 l^2 s^2 + m_V l K_\varphi = 0$$

It can be seen from this equation that the $K_{\dot{\varphi}}$ gain, in the coefficient of s, of drive system control will supply damping to the system, and the K_φ gain

will increase the pendulum frequency so as to keep the bridge above the suspended vehicle.

The bridge drive unit was an electro-hydraulic unit consisting of a synchronous electric motor which drove a variable displacement hydraulic pump. Control of the bridge was exercised by the operation of a pump stroker, which controlled the displacement of this pump. The pump drove the fixed displacement hydraulic motors attached to the wheels of the bridge. A fixed displacement of the stroker produced a steady state constant velocity of the bridge.

Since the stroker controlled bridge velocity instead of bridge acceleration, the control function of accelerating the bridge as a function of pendulum angle was achieved by displacing the stroker as a function of the integral of the pendulum angle, and the function of accelerating the bridge as a function of rate of change of pendulum angle was achieved by displacing the stroker as a function of pendulum angle.

The predominant dynamic characteristic of the drive unit was the oscillatory response of bridge velocity to stroker displacement that resulted from the compressibility of the hydraulic fluid as it reacted against the mass of the bridge. This dynamic characteristic is expressed by the equation

$$\frac{\dot{x}_B}{\text{Stroker displacement}} = \frac{\dfrac{c_1}{d_m}}{\dfrac{B}{V}\dfrac{J_L}{d_m^2}s^2 + \dfrac{J_L K_L}{d_m^2}s + 1}$$

where

c_1 oil volume delivered by pump per unit displacement of stroker, in^3/unit

d_m motor displacement, 28 in^3/rad

B bulk modulus of oil, 1×10^5 psi

V oil volume under compression, 600 in^3

J_L total inertia of load reflected at motor output shaft, 3050 in-lb/sec^2

K_L leakage coefficient, in^3/sec/psi

For the system under study, the natural frequency of the drive unit as determined by this equation is 4.6 rad/sec. The detailed analysis of the system naturally included this characteristic.

In addition to the drive unit dynamics, the following dynamic factors were also included in the detailed analysis

    (1) the compliance of the primary electric motor

    (2) the time constant and the limit displacement of the stroker

    (3) the motor leakage, as a function of $\sqrt{\text{pressure}}$

    (4) pressure relief valve flow

    (5) nonlinear friction of the gearing

    (6) tire compliance

Another important dynamic characteristic of the system was the oscillatory characteristic of the cable. Cable vibrations added to the measured cable angle and therefore added a spurious signal to the control signal. Equations for the first two modes of vibration for different, fixed cable length were determined and used in the analysis. These equations included the effect of a lumped mass located near the vehicle which represented the whiffletree which was a part of the support and gimbal arrangement of the vehicle. The frequency of the first mode for a 200-foot cable length was 8.72 rad/sec, which is very close to the natural frequency of the drive unit, and which therefore put a limit on the precision with which the bridge could be maintained above the vehicle. This vibration frequency would increase at shorter cable lengths, and also change with vehicle weight. The analysis was made for fixed cable lengths and vehicle weights.

6

Pilot Transfer Function

The pilot transfer functions, which were used in conjunction with the simulator equations, are derived in reference 1 and are repeated here. The pilot-vehicle system involved in the landing maneuver is a multiloop system described in the block diagram presented in figure 1. The inner loop deals with the attitude control of the vehicle. The vehicle response to attitude control was assumed to contain a proportional rate feedback, and is given by the equation

$$\frac{\theta}{\delta} = \frac{0.5}{s(s + 0.5)}$$

which defines a rate system with a rate response with a time constant of 2 seconds. Reference 1 demonstrates that a pilot's response in such an inner loop is given by

$$\frac{\delta}{\theta_{c,e}} \approx \frac{K_1 \tau \left(1 + \frac{K_2}{\tau} s\right)}{(s + \tau)^2} = \frac{96(1 + 0.4s)}{(s + 6)^2}$$

The combination of the pilot and vehicle gives this inner loop a closed-loop characteristic frequency of 1.2 rad/sec and a damping ratio of 0.26.

The outer loop of the system deals with the longitudinal translation, and the vehicle response to attitude angle is given by a pure inertial response

$$\frac{x}{\theta} = \frac{5.36}{s^2}$$

This relation is derived from the linearized equation of motion for the horizontal component of acceleration due to one-sixth of thrust that would be in effect in the lunar environment

$$\ddot{x} = \frac{1}{6}g \sin\theta$$

using small angle linearization

$$\ddot{x} = \frac{1}{6}g\theta = 5.36\theta \text{ ft/sec}^2 = 1.63\theta \text{ m/sec}^2$$

$$\frac{\ddot{x}}{\theta} = 5.36 \frac{\text{ft/sec}^2}{\text{rad}} = 1.63 \frac{\text{m/sec}^2}{\text{rad}}$$

Reference 1 demonstrates that the pilot response in such an outer loop is

$$\frac{\theta_c}{x_e} = \frac{0.9(1 + 9.2s)}{(s + 10)^2}$$

This pilot response defines a characteristic response of the complete system which has two small real roots, $s = -0.167$ and $s = -0.336$. In terms of an oscillatory response, these two roots define an overdamped response with a natural frequency given by

$$\omega = \sqrt{(0.167)(0.336)} = 0.236 \text{ rad/sec}$$

This system frequency characterizes the translation response of the system. Since the response characteristic of the longitudinal drive system of the simulator must have a response frequency higher than that of the system which is to be tested, this calculated response characteristic of the pilot controlled translation response provides a first, rough criterion for the required characteristics of the longitudinal drive system.

ANALYSIS AND TEST RESULTS

A detailed analytical study was made to determine precisely the drive system characteristics and the suitability of the characteristics. The computer

8

diagram used in this study is presented in figure 2. It includes the complete representation of the drive system, the cable dynamics, and the pilot controlled vehicle representation.

The first phase of the study was conducted to determine just how fast the bridge could be made to respond. Open-loop step thrust inputs to the vehicle were used as the forcing function in these studies. The results showed that the presence of the cable vibration modes of motion in the system placed an upper limit on the pendulum damping gain $K_{\dot{\phi}}$. If this gain was adjusted too high, the first vibration mode would become unstable, as is illustrated in figure 3.

The limit on the pendulum damping gain placed further restriction on the pendulum frequency gain K_{ϕ}. The range of possible system characteristics that could be achieved is shown in figure 4, which shows the vehicle velocity response to a 2-second thrust impulse. The oscillatory nature of these responses is the result of the bridge drive system characteristics. It can be seen that a well-damped response with a frequency of 1.57 radians/sec (a period of 4 seconds), or a poorly damped response with a frequency of 2.5 rad/sec (a period of 2.5 seconds) could be achieved.

Both of these frequencies are above the 0.236 rad/sec frequency for the pilot controlled translation response of the lunar landing system. However, it cannot be confidently concluded that they are sufficiently high so as to have no effect on the simulation. To determine what effect the bridge response might have on the pilot-controlled maneuver, the analytical representation of the pilot and vehicle were included in a closed-loop representation of the complete system, and the response to a commanded 200-foot displacement was determined. The results are presented in figure 5, which show, first, the

response of the pilot-vehicle combination alone, and then the response of the pilot-vehicle-simulator combination with the two different simulator character-istics presented before. Using the pilot-vehicle combination response as the standard for comparison it can be seen that including the simulator bridge dynamics in the loop does indeed influence the response. With the lower gain bridge control the system is degraded to the point of instability. It was therefore concluded that the simulator should be adjusted so as to have as high a frequency characteristic as possible. Also, it was indicated by the analysis that the pilots might find the simulator slightly more difficult to control than the real lunar landing system.

Post-Analysis Tests

When the simulator was put in operation, the system characteristics which could be achieved with the actual mechanism were determined. It was found that the highest stable pendulum frequency that could be obtained was 1.4 rad/sec (a period of 4.5 seconds). Piloted runs were then made with this highest fre-quency response of the bridge, and with the K_φ gain placed at a lower setting to check the analytical results that such a change would affect the piloted system response. The lower frequency used was approximately 0.8 rad/sec (a period of 8 seconds). Figure 6 shows cable angle responses of the simulator in these two conditions to open-loop step impulses. The piloted tests were started with the vehicle hovering at an altitude of approximately 30 feet. The pilot then translated the vehicle 200 feet and attempted to stop and hover over a mark located on the ground. The run with the higher response was made first, and then immediately a second run was made with the lower setting. Two differ-ent pilots were used.

Sample time histories of these tests are shown in figure 7. In this test the first maneuver, from the 50-foot point to the 275-foot point, was done with the high-gain drive system. At the 50-second mark, while the pilot was turning 180°, the drive system gain was readjusted to the low-gain setting, and the pilot started to go back to the 50-foot mark. It can be seen that the general nature of these maneuvers is very similar to that computed in the analytical study. With the lower response characteristics for the simulator a very noticeable decrease in damping of the attitude angle can be seen. The pilot did not continue the maneuver in this case, but rather dropped the intention to precisely control translation. He stopped the attitude oscillation and landed at the point that was below him at that time. The pilots commented that in the lower response runs they were having more difficulty in controlling the vehicle, and as one pilot said, he felt he was in a "pilot-induced oscillation" condition.

Since the simulator characteristics that were achieved with the actual mechanism when it was put in operation were not the same as those determined in the analytical study, and since the pilot's response showed a lower attitude angle limit in the flight tests than was assumed in the analytical study, the analytical study was repeated in an attempt to reproduce more closely the flight time histories. In these repeated calculations the drive system gains were adjusted to give a poorly damped 4.5-second pendulum period in one case and a well damped 8-second pendulum period in the second case to correspond to the two conditions that were tested in the flight tests. The same linear transfer functions were used for the representation of the pilot. The attitude limit was placed at 10°, which corresponds more closely with the limit used by the pilot in the flight tests than did the 40° limit used in the initial analytical study.

With this 10° limit on attitude angle, a well-controlled attitude time history was calculated, shown in figure 8(a), which is a better reproduction of the flight time history than was the initially calculated response. When the simulator characteristics were changed so as to have an 8-second period, a deterioration in the stability of the calculated attitude angle time history resulted. These repeated calculations further confirm the conclusion drawn from the initial analytical study.

CONCLUSIONS

The experience gained in the exercise of predicting the characteristics of a manually controlled simulator and verifying these characteristics when the simulator was put in operation has demonstrated the validity and usefulness of analytical expression of human response. The analysis showed that the range of simulator dynamics which was likely to occur in the simulator would influence the response of the pilot-controlled maneuver, and tests with the completed hardware confirmed this conclusion.

It was concluded that the gain of the simulator longitudinal drive system should be kept as high as possible to minimize the effect on the piloted maneuvers, and it was indicated by the analysis that the tasks performed with the simulator might be slightly more difficult than the same tasks performed in the lunar environment.

REFERENCE

1. Adams, James J.; Bergeron, Hugh P.; and Hurt, George J.: Human Transfer Functions in Multi-Axis and Multi-Loop Control Systems. NASA TN D-3305, April 1966.
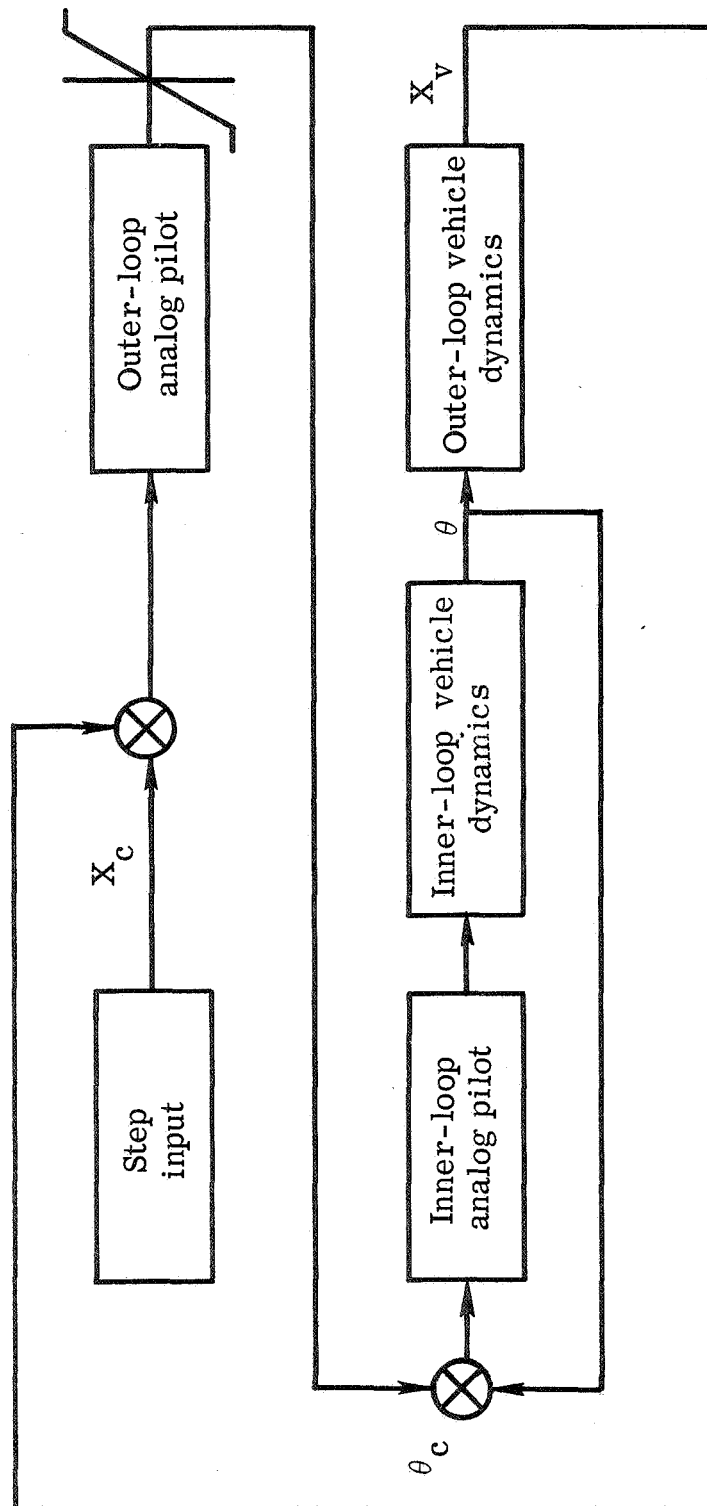
Figure 1.- Block diagram of the double control loop.
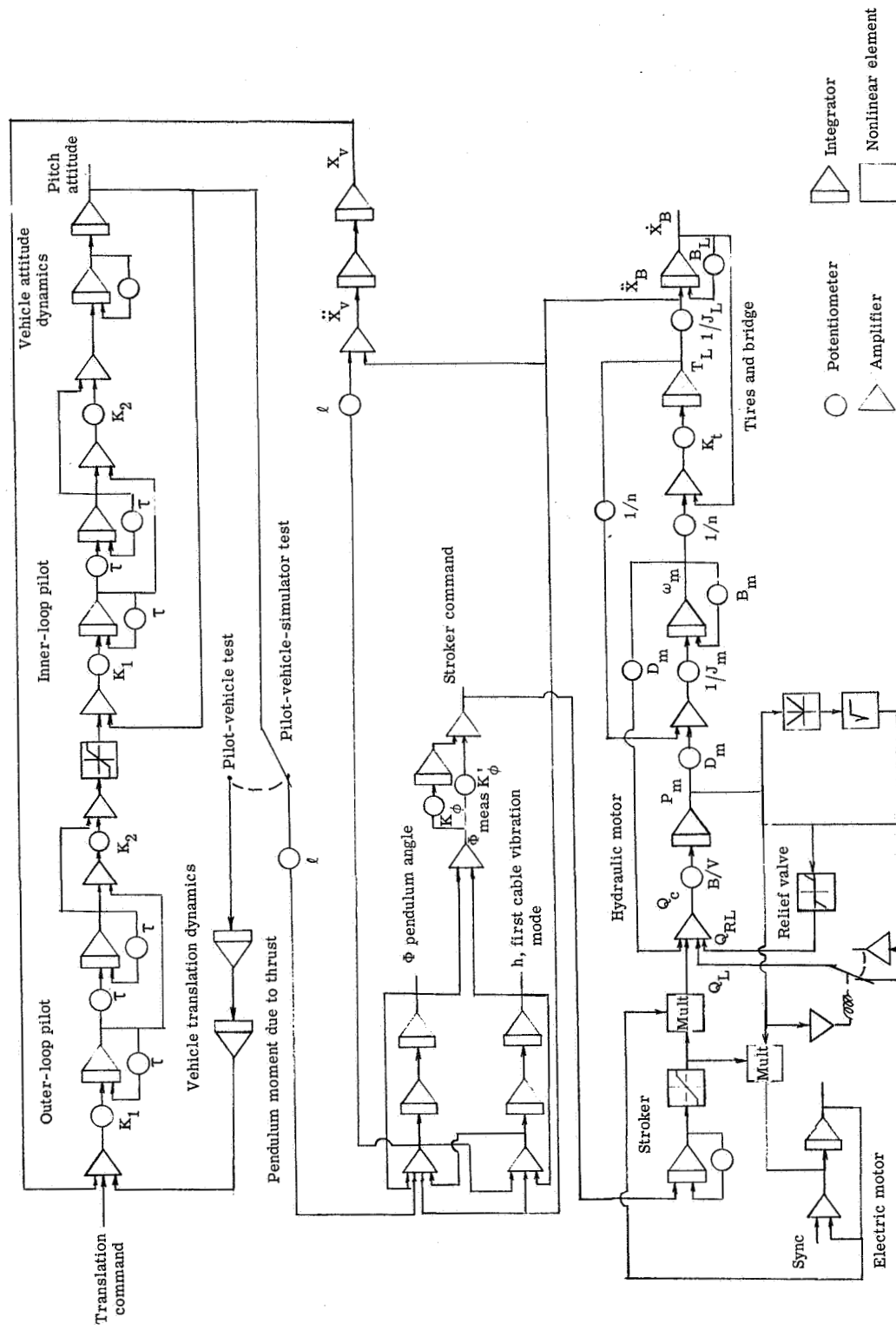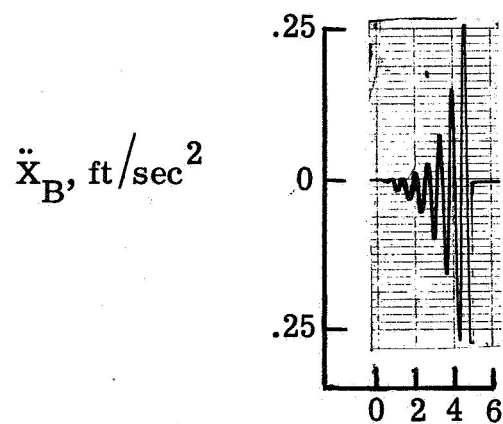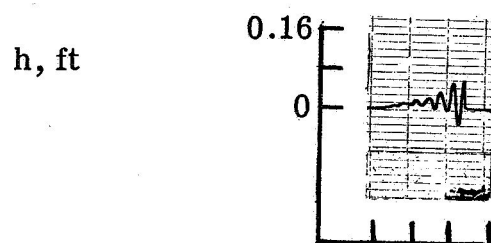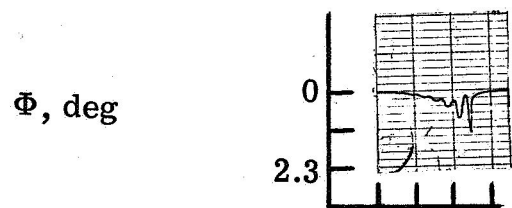
Figure 2.- Diagram of pilot-vehicle-simulator system.
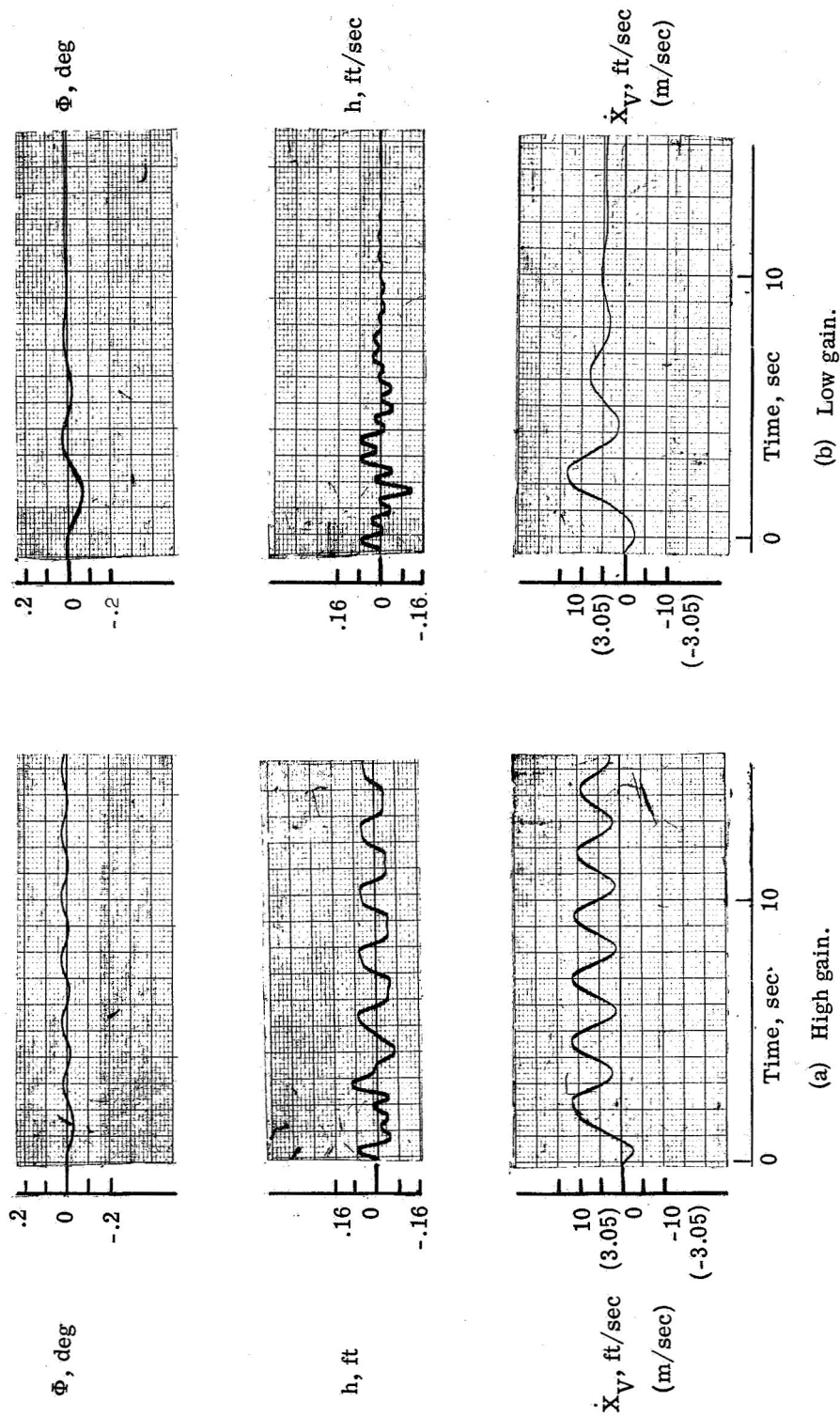
Figure 3.- Calculated cable divergence.

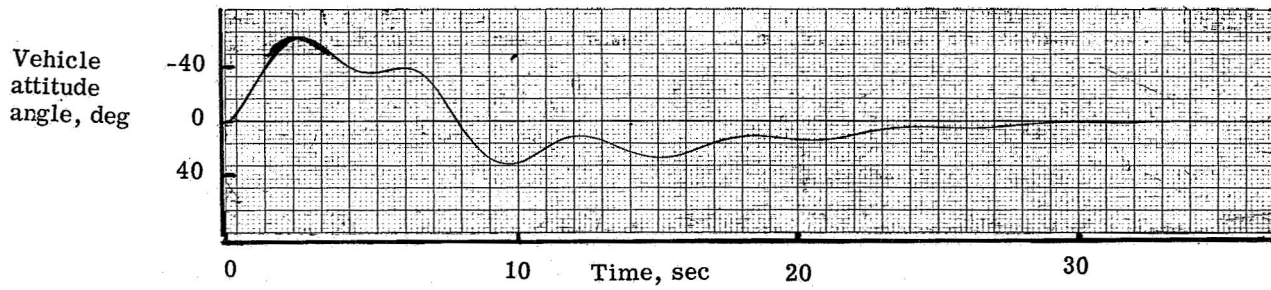Figure 4.- Calculated response of simulator to a 2-second thrust impulse.

Vehicle
attitude
angle, deg

-40

0

40

0   10   Time, sec   20   30

(a) Pilot vehicle combination.

Vehicle
attitude
angle, deg

-40

0

40

0   10   Time, sec   20   30
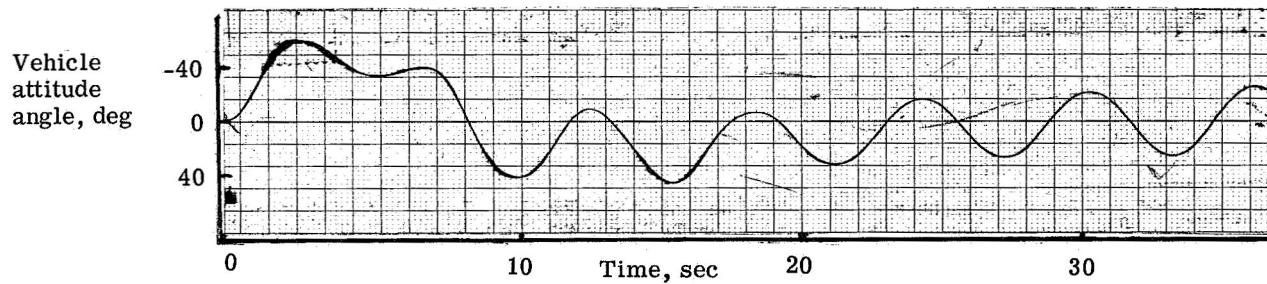
(b) Pilot-vehicle-simulator combination with
high gain simulator.

Vehicle
attitude
angle, deg

-40

0

40

0   10   Time, sec   20   30
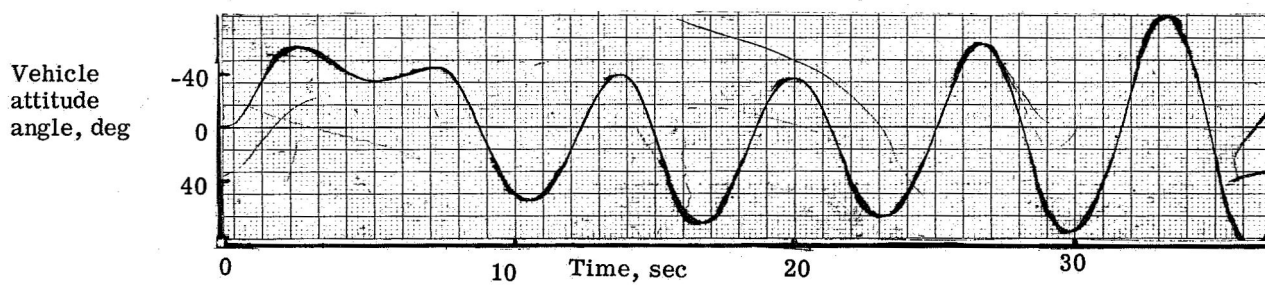
(c) Pilot-vehicle-simulator combination with
low gain simulator.

Figure 5.- Calculated vehicle attitude response to a 200-foot step
translation command.
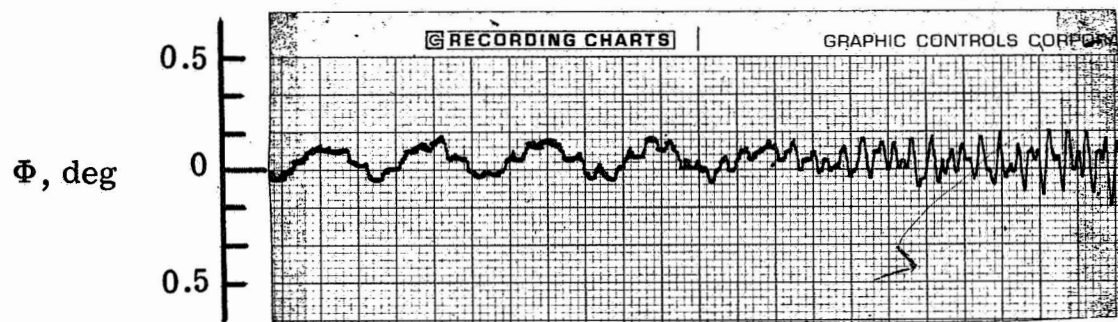
(a) High gain.
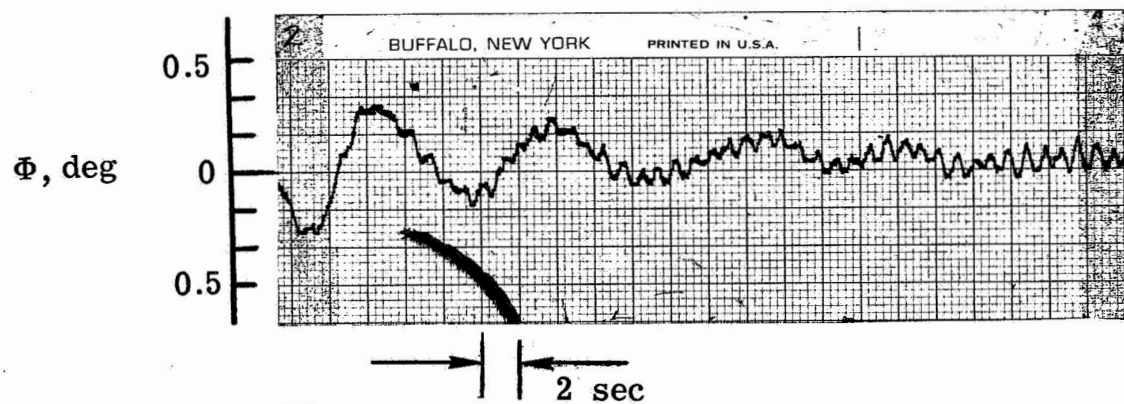
(b) Low gain.

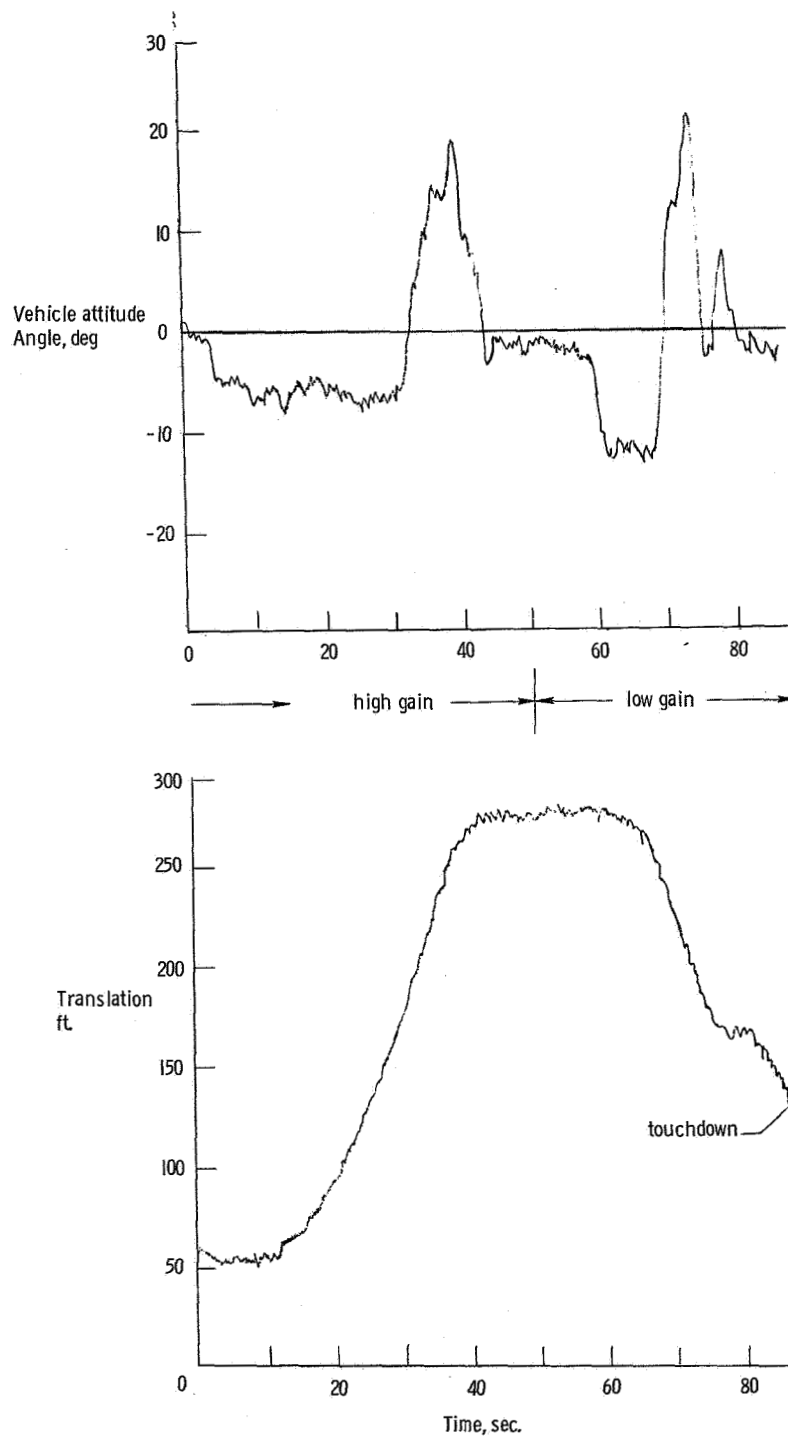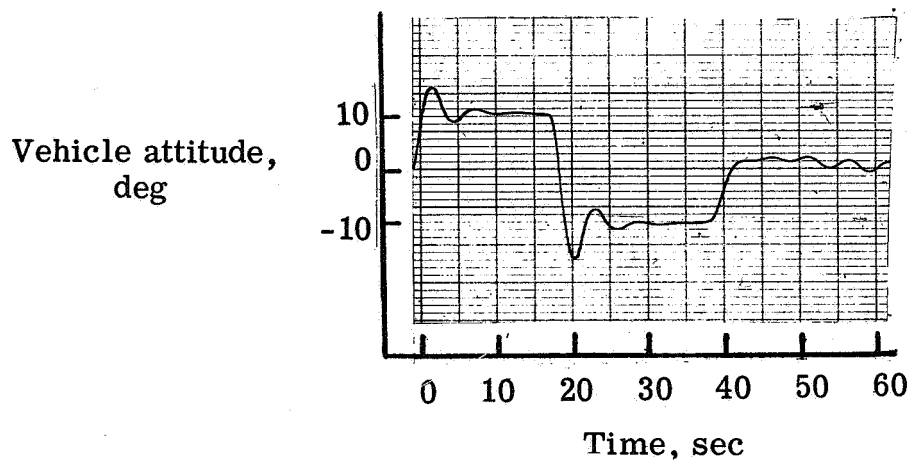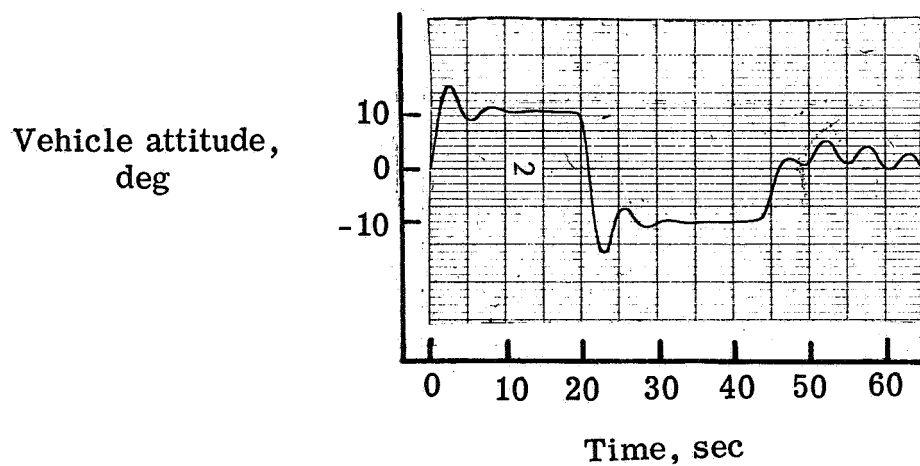Figure 6.- Simulator cable angle response to small inputs.

Figure 7.- Simulator response to a 200-foot
translation command with both high gain
and low gain simulator control.

Vehicle attitude,
deg

(a) Pilot-vehicle-simulator combination with low gain
(4 second period) simulator.

Vehicle attitude,
deg

(b) Pilot-vehicle-simulator combination with very low
gain (8 second period) simulator.

Figure 8.- Repeated calculation of vehicle attitude response to a
200-foot step translation command.